ARTICLES

Gap junction adhesion is necessary for radial migration in the neocortex

Laura A. B. Elias[1,2], Doris D. Wang[1,2] & Arnold R. Kriegstein[2]

Radial glia, the neuronal stem cells of the embryonic cerebral cortex, reside deep within the developing brain and extend radial fibres to the pial surface, along which embryonic neurons migrate to reach the cortical plate. Here we show that the gap junction subunits connexin 26 (Cx26) and connexin 43 (Cx43) are expressed at the contact points between radial fibres and migrating neurons, and acute downregulation of Cx26 or Cx43 impairs the migration of neurons to the cortical plate. Unexpectedly, gap junctions do not mediate neuronal migration by acting in the classical manner to provide an aqueous channel for cell–cell communication. Instead, gap junctions provide dynamic adhesive contacts that interact with the internal cytoskeleton to enable leading process stabilization along radial fibres as well as the subsequent translocation of the nucleus. These results indicate that gap junction adhesions are necessary for glial-guided neuronal migration, raising the possibility that the adhesive properties of gap junctions may have an important role in other physiological processes and diseases associated with gap junction function.

During neocortical brain development, radial glia, which reside in the ventricular zone and extend a fibre to the pial surface, serve two purposes: (1) as stem cells of the developing cortex, giving rise to neurons[1,2], and (2) as guides along which the neurons migrate to reach the correct lamina of the cortical plate, where they will become pyramidal cells in the adult cortex[3–5]. Interstitial junctions containing filamentous material have been found between migrating neurons and radial fibres, suggesting a close association between the two cell types[6–8].

The molecules that mediate the critical interaction between the radial glial fibre and the migrating neuron remain largely unknown. Astrotactin has been described as an adhesion molecule in the cerebellar cortex[9,10], but has not been implicated in neocortical development. Neuregulin and its soluble form, glial growth factor, mediate bi-directional signalling between the radial fibre and the migrating neuron, and are important for radial glial maintenance and neuronal migration[11]. $\alpha_3\beta_1$ integrin expressed in migrating neurons is involved in glial recognition, and α_V integrin expressed in radial glia is involved in neuronal adhesion[12]. The expression of gap junctions in radial fibres and migrating neurons, together with the detection of gap junctions between nestin$^+$ radial glial fibres and nestin$^-$ cells by electron microscopy, suggests the possibility that gap junctions play a part in neuron–glial interactions and neuronal migration[13]. This hypothesis is supported by the change in the distribution of bromodeoxyuridine (BrdU) pulse-labelled cells in the *Cx43* genetic knockout (*Cx43*KO)[14]. Furthermore, strong evidence links Cx43 to migration in neural crest cells and gliomas; however, the mechanisms are not fully understood[15–18].

Gap junctions are large-diameter channels made up of two hemichannels—each composed of six connexin subunits—on opposing membranes that join through hydrophobic interactions and form an aqueous pore between the cytoplasm of two adjacent cells[19]. The gap junction subunits expressed in the developing cortex include Cx26 (also known as Gjb2), a β1 connexin family member, and Cx43 (also known as Gja1), an α1 connexin family member[20]. There is strong evidence that radial glia are coupled electrically and chemically to each other by gap junction channels during embryonic development[21]. Functionally, it has been suggested that gap junctions have a role in radial glial cell cycle regulation because pharmacological block of gap junctions, or Ca^{2+} waves mediated by gap junction hemichannels, inhibits the cell cycle[22,23]. However, the possible role of gap junctions in cortical migration remains largely unexplored.

Gap junction expression at contact points

The gap junction subunits Cx26 and Cx43 are expressed in the developing rat neocortex. Whereas Cx26 is evenly distributed from the ventricular zone through the intermediate zone to the cortical plate, Cx43 is highly expressed at the ventricular surface and its levels are reduced in the cortical plate (Fig. 1a, b, e, f). Cx26 and Cx43 puncta do not colocalize with each other (Supplementary Fig. 1), because they belong to separate families that do not make heterotypic junctions or heteromeric hemichannels[24]. The expression of both connexins outside of the ventricular zone proliferative region indicates that gap junctions may regulate functions additional to radial glial proliferation. To address this possibility, we determined the pattern of Cx26 and Cx43 expression with respect to β-III tubulin$^+$ migrating neurons and vimentin$^+$ radial glial fibres. Both gap junction subunits are expressed in migrating neurons and along radial fibres. In fact, Cx26 and Cx43 are highly localized in neurons to the regions of contact with radial fibres, consistent with the idea that gap junctions may have a role in mediating communication between migrating neurons and their radial guides (Fig. 1, and Supplementary Movies 1, 2).

Cx26 and Cx43 are necessary for migration

To investigate the role of gap junctions in cortical development, we developed acute loss-of-function manipulations for each connexin using RNA interference. Short hairpin RNA (shRNA) constructs that produced significant knockdown of rat Cx26 or Cx43 by western blot in Cos-7 monkey cells were selected (*Cx26*-shRNA or *Cx43*-shRNA, respectively), and it was confirmed that the same hairpin sequences with three point mutations (Ctrl-shRNA) failed to produce significant knockdown (Supplementary Fig. 2a, b). We confirmed that

[1]Neuroscience Graduate Program, [2]Institute for Regeneration Medicine, University of California San Francisco, 513 Parnassus Avenue, San Francisco, California 94143, USA.

Cx26-shRNA and *Cx43*-shRNA were able to knockdown endogenous connexin protein in the developing rat brain (Supplementary Fig. 2c, d).

We next examined the functional effects of Cx26 or Cx43 down-regulation in the intact developing neocortex. *In utero* intraventricular injection and electroporation of *Cx26*-shRNA or *Cx43*-shRNA at embryonic day (E)16 resulted in a striking cellular redistribution pattern compared with Ctrl-shRNA at E18 and E21 (Fig. 2a). We quantified this effect by dividing the cortex into five equal areas and determining the fraction of the total number of shRNA-expressing (GFP$^+$) cells in each area (Fig. 2b). At E18, there was a significant change in the fraction of cells in all areas except in the ventricular zone; most clearly there was a loss of cells in the lower and upper cortical plate (Fig. 2b). The effect was more dramatic at E21; the percentage of cells in each area, except the ventricular zone/SVZ (sub-ventricular zone), was significantly different. Most strikingly, there was an accumulation of cells in the intermediate zone, with far fewer cells in the cortical plate (Fig. 2b). The intermediate phenotype of the *Cx26*-shRNA is due to a rostral caudal gradient such that *Cx26*-shRNA exerts a stronger effect on neuronal migration in caudal regions where Cx26 is highly expressed (Supplementary Fig. 3). The target-specificity of these results was confirmed by using alternative shRNA targets for Cx26 and Cx43 (Supplementary Fig. 4).

Because radial glia express connexins, it was possible that the defect in neuronal migration was due to a disruption in the radial glial scaffolding. However, immunohistochemical analysis of the radial glia, as well as the migration of wild-type neurons in electroporated regions, seemed normal (Supplementary Fig. 5). To address this possibility further, transplant assays were performed. Brains were

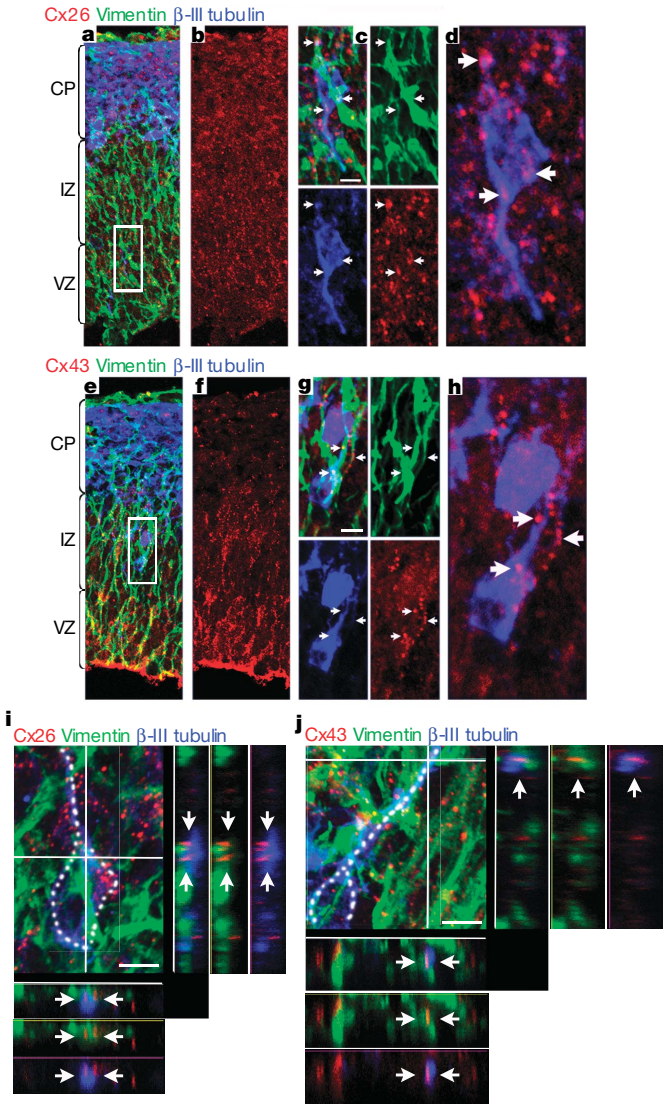

Figure 1 | Cx26 and Cx43 are localized to contact points between migrating neurons and radial glial fibres. **a**, **e**, Immunohistochemistry of cortical sections at E16 showing overlay of Cx26 (**a**) or Cx43 (**e**) (red), vimentin (green) to label radial fibres, and β-III tubulin (blue) to label immature neurons. **b**, **f**, Red channel of panels **a** and **e** showing expression pattern of Cx26 (**b**) or Cx43 (**f**). **c**, **g**, Migrating neuron from boxed area of panels **a** and **e**; clockwise: overlay, vimentin (green), Cx26 (**c**) or Cx43 (**g**) (red), and β-III tubulin (blue). Cx26 and Cx43 are expressed in neurons and radial glia (white arrows). **d**, **h**, Overlay of Cx26 (**d**) or Cx43 (**h**) and β-III tubulin in migrating neuron (from panels **c** and **g**). **i**, **j**, 'High resolution' confocal stacks highlighting the relationship between Cx26 (**i**) or Cx43 (**j**) puncta, vimentin$^+$ fibres and a β-III tubulin$^+$ neuron (dotted outline). Cross sections through the *x* and *y* axis, bottom and right panels, respectively, show individual connexin puncta (white arrows) at the interface between the vimentin$^+$ radial fibre and β-III tubulin$^+$ migrating neuron (Supplementary Movies 1 and 2 provide three-dimensional rotations). Scale bars, 5 μm. CP, cortical plate; IZ, intermediate zone; VZ, ventricular zone.

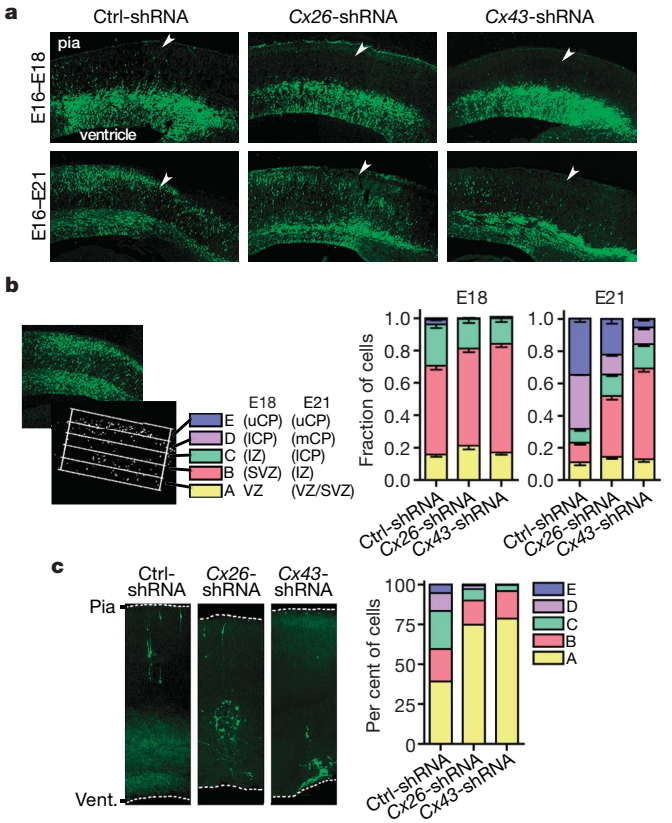

Figure 2 | Knockdown of Cx26 or Cx43 impairs neuronal migration. **a**, Coronal sections from brains electroporated at E16. *Cx26*-shRNA or *Cx43*-shRNA reduces the fraction of cells in the cortical plate (white arrows) at E18 and E21. **b**, Quantification of shRNA knockdown-mediated cell distribution effect. Left panels, representative optical section with grid overlay of five equal areas (A–E) and quantification threshold. Right panels show a significant change in the distribution of cells in all areas except A at E18 and E21 (1-way ANOVA, E18: A, $P = 0.0745$; B, $P = 0.0010$; C, $P = 0.0106$; D, $P \leq 0.0001$; E, $P < 0.0001$; E21: A, $P = 0.3625$; B, $P \leq 0.0001$; C, $P = 0.0003$; D, $P \leq 0.0001$; E, $P \leq 0.0001$; $n = 3$ brains per condition). Values represent mean ± s.e.m. **c**, Connexin expression in neurons is necessary for migration. Ctrl-shRNA-expressing cells transplanted into a wild-type host brain are able to integrate and migrate, whereas transplanted *Cx26*-shRNA- or *Cx43*-shRNA-expressing cells have reduced migration capacity (Chi-square, Ctrl-shRNA versus connexin-shRNA: A, $P < 0.0001$; B, $P < 0.0001$; C, $P > 0.05$; D, $P < 0.0001$; E, $P < 0.0001$; Ctrl-shRNA, $n = 225$ cells; *Cx26*-shRNA, $n = 421$; *Cx43*-shRNA $n = 698$). The pial surface (pia) and ventricle (vent.) are labelled to indicate orientation.

electroporated at E16 and shRNA-expressing (GFP^+) cells were microdissected and intraventricularly injected into wild-type brains at E17. In contrast to donor Ctrl-shRNA expressing cells, which were able to engraft and migrate towards the upper layers of the cortex, the *Cx26*-shRNA- and *Cx43*-shRNA-expressing donor cells were able to engraft into the host brain but had a significantly reduced migration capacity (Fig. 2c). These data suggest that connexin expression in neurons is required for migration.

We next examined secondary defects potentially able to affect cell distribution independent of migration. Neurons expressing *Cx*-shRNA were able to exit the cell cycle and begin to differentiate normally (Supplementary Fig. 6a, b). Furthermore, terminal transferase dUTP nick end labelling (TUNEL) staining showed no change in apoptosis (Supplementary Fig. 6c). Additionally, the expression pattern of N-cadherin, zona occludens-1 and β_1-integrin seemed unchanged, suggesting that connexin knockdown does not overtly disrupt expression of other cell–cell adhesion proteins (Supplementary Figs 7, 8). Together these data suggest that the defect in migration is not secondary to a defect in cell cycle exit, differentiation, cell death, or downregulation of other adhesion proteins.

Adhesions, not channels, mediate migration

What is the mechanism by which gap junctions mediate neuronal migration? We sought to differentiate among three plausible functions. Gap junctions can electrically and chemically couple cells to allow the exchange of current or small molecules, mediate extracellular release of substrates such as ATP through hemichannels, or provide an adhesive contact between two cells. We performed selective rescue experiments to distinguish these possibilities.

First, to rescue the migration phenotype, conservative mutations (CM) were introduced into the shRNA-targeted regions of Cx26 or Cx43 (Cx26CM or Cx43CM respectively), which prevented shRNA-induced knockdown (Supplementary Fig. 9). These constructs, or enhanced yellow fluorescent protein (EYFP) alone, were electroporated with the shRNA constructs at a set molar ratio. The co-expression of Cx43CM or Cx26CM with its respective shRNA construct significantly rescued the fraction of cells that migrate to the cortical plate, demonstrating the target-specificity of the shRNA effect (Fig. 3).

To determine whether functional channels are necessary to rescue the migration defect, a conserved tyrosine in the third transmembrane domain of Cx26 and Cx43 was mutated (Cx26CMT135A or Cx43CMT154A, respectively). These dominant-negative connexin mutants are able to make adhesions but have a closed channel and thus are not able to mediate exchange between cells or with the extracellular environment[25] (Supplementary Figs 10, 11). Remarkably, these mutants rescued the migration of cells to the cortical plate (Fig. 3). The ability of the closed channel mutants to rescue the migration defect strongly suggests that the channel (either hemichannel or gap junction channel) does not contribute to the role of gap junctions in neuronal migration.

It has been shown that Ca^{2+} is important for neuronal migration[26] and that gap junctions mediate Ca^{2+} waves in the developing cortex by releasing ATP through hemichannels that activates purinergic P2Y1 receptors on radial glia[23]. Thus, to further test the possibility that hemichannel-mediated Ca^{2+} waves have a role in neuronal migration, Ca^{2+} waves were inhibited by pharmacologically antagonizing the P2Y1 receptor with suramin or by knocking down the P2Y1 receptor with multiple shRNA constructs. No migration defect was observed, suggesting that hemichannel-mediated Ca^{2+} waves are not involved in cortical neuronal migration (Supplementary Fig. 12).

To determine whether the adhesive properties of gap junctions are necessary for migration, one of the conserved extracellular cysteines

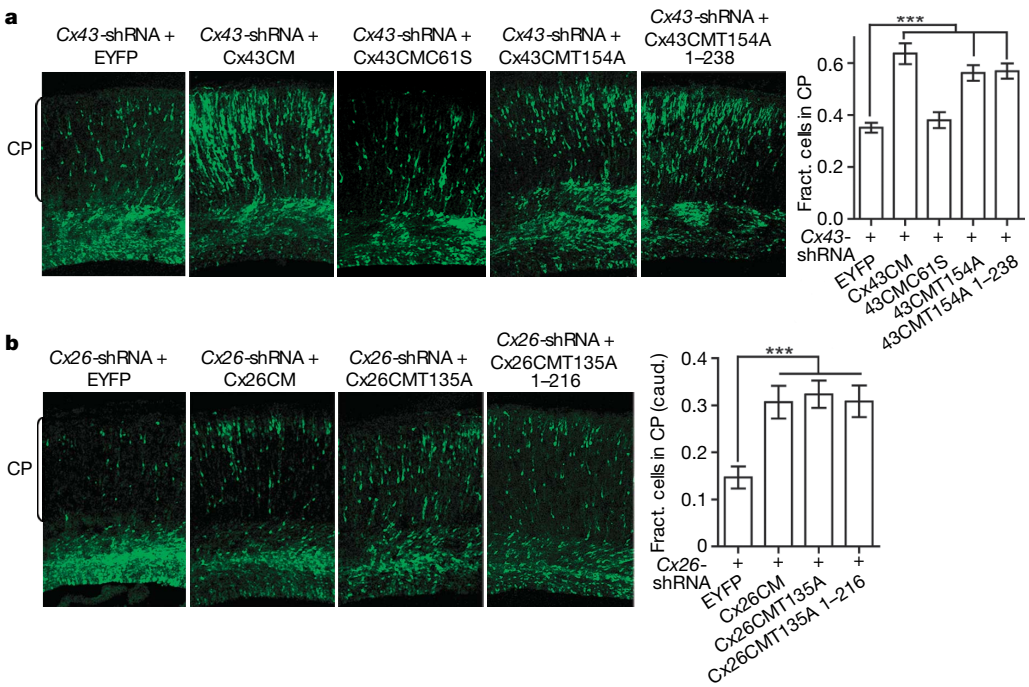

Figure 3 | Rescue of connexin-shRNA induced migration phenotype by wild-type connexin and connexin mutants that make adhesions but not channels. **a**, Cx43CM (function: channel, adhesion, C terminus), Cx43CMT154A (function: adhesion, C terminus), or Cx43CMT154A 1–238 (function: adhesion) significantly increased the fraction of cells in the cortical plate compared to EYFP when co-expressed with *Cx43*-shRNA (***$P < 0.0001$, *t*-test; EYFP, $n = 6$ brains; Cx43CM, $n = 4$; Cx43CMT154A, $n = 5$; Cx43CMT154A 1–238, $n = 6$). Cx43CMC61S (function: hemichannel, C terminus) did not rescue the migration defect (EYFP versus Cx43CMC61S, *t*-test $P = 0.4727$; Cx43C61S, $n = 4$ brains). **b**, Cx26CM (function: channel, adhesion, C terminus), Cx26CMT135A (function: adhesion, C terminus), or Cx26CMT135A 1–216 (function: adhesion) significantly increased the fraction of cells in the cortical plate compared to EYFP when co-expressed with *Cx26*-shRNA (***$P \leq 0.0001$, *t*-test; EYFP, $n = 4$ brains; Cx26CM, $n = 5$; Cx26CMT135A, $n = 5$; Cx26CMT135A, 1–216, $n = 5$). For 26-shRNA rescue, only caudal (caud.) sections (as described in Methods) were used, because the migration phenotype is stronger caudally (Supplementary Fig. 3). Values represent means ± s.e.m.

was mutated (Cx43CMC61S) to produce a Cx43 channel that does not make adhesions and thus cannot form gap junctions[17], but maintains the ability to make functional hemichannels (Supplementary Figs 10, 11). Interestingly, Cx43CMC61S failed to rescue the *Cx43*-shRNA-induced migration defect, suggesting that the adhesive properties of gap junctions are necessary for radial migration (Fig. 3a).

In addition, we wanted to determine whether signalling by carboxy-terminal interactions with cytosolic proteins are important. Cx26 has a short, uncharacterized intracellular C terminus, whereas Cx43 has a longer C terminus, which interacts with a variety of proteins including zona occludens-1, V-Src, and tubulin[27–29]. Both C-terminal truncations of the closed channel mutants (Cx43CMT154A 1-238 and Cx26CMT135A 1-216) were able to rescue the migration defect (Fig. 3). These results suggest that signalling mediated by the cytoplasmic C termini does not have a significant role during migration. However, the possibility remains that intermolecular interactions with other parts of the connexin protein may be important. In summary, we found that adhesion, but not the channel or the C terminus, is necessary for the role of gap junctions during neuronal migration.

Gap junctions provide adhesion

To demonstrate that gap junctions can mediate adhesion in cortical cells, we built on previous work showing that overexpression of Cx43, but not Cx43C61S, increases adhesion in C6 glioma cells[17]—a cell type without endogenous gap junction expression[30]. We used C6 cells with or without stable transfection of Cx43–EYFP[31] to provide a glial substrate on which we could place embryonic cortical cells and test their ability to adhere. Cortical cells were electroporated with Ctrl-shRNA, dissected and FACS-sorted for GFP, labelled with DiD, and plated on C6 cells or C6 cells expressing Cx43–EYFP (C6 + Cx43). We found a twofold increase in the number of DiD^+ cells adhering to the C6 + Cx43 substrate compared with the C6 substrate, suggesting that cortical cells can use endogenous Cx43 as a means of cell–cell adhesion (Fig. 4a).

To test whether *Cx43*-shRNA reduces the ability of cortical cells to adhere to the C6 + Cx43 substrate, Ctrl-shRNA or *Cx43*-shRNA FACS-sorted cells were plated on C6 cells or C6 + Cx43 cells. There was a significant reduction in the ratio of the number of *Cx43*-shRNA to Ctrl-shRNA cells on the C6 + Cx43 substrate compared with the C6 substrate (Fig. 4b). Thus, we show that cortical cells can use endogenous Cx43 to adhere to a glial substrate and that knocking down Cx43 reduces their ability to adhere to a Cx43-expressing substrate, but not a control substrate.

Classical adhesion molecules typically provide a link with internal cytoskeletal components. Previous work in neural crest cells demonstrates that Cx43 colocalizes and co-immunoprecipitates with numerous actin-binding proteins, and that filamentous actin is disorganized in neural crest cells from the Cx43 knockout mouse[32]. To explore connexin–actin interactions, actin tagged with the red fluorescent protein cherry (actin–cherry) was co-electroporated with GFP. Electroporated actin is diffusely distributed in radial glia and newborn neurons and becomes punctate in multipolar SVZ cells and migrating neurons (Supplementary Fig. 13). Co-electroporation of Cx26T135A or Cx43T154A (to avoid toxicity associated with overexpression of wild-type connexin; Supplementary Fig. 11) with actin–cherry revealed that both Cx26 and Cx43 puncta frequently colocalize with the actin puncta, with the connexin puncta slightly offset (Fig. 4c). Interestingly, cells expressing *Cx26*-shRNA or *Cx43*-shRNA, have significantly fewer actin puncta than Ctrl-shRNA-expressing cells (Fig. 4d). This suggests that both Cx26 and Cx43 can interact with the actin cytoskeleton.

Connexin dynamics during migration

To investigate the dynamic behaviour of migrating neurons, we performed time-lapse live imaging. We observed that control migrating neurons typically start with a bifurcated leading process, one branch of which prevails, and the neuron's soma then translocates forward into a dilation that forms in this leading process[33] (Fig. 5a, Supplementary Movie 3). Interestingly, migrating neurons with multiple leading processes can show differential expression of Cx43 or Cx26 in these processes (Fig. 5b). Hence, we hypothesized that gap junction adhesions play a part in stabilizing the leading process along a radial glial fibre. Indeed, *Cx43*-shRNA- and *Cx26*-shRNA-expressing neurons are unable to stabilize their processes and continue to extend multiple branches (Fig. 5c, Supplementary Movie 4, 5). This phenotype is reminiscent of neural crest cells from *Cx43*KO mice that show increased protrusive activity but decreased directional migration[32].

To analyse the dynamics of connexin puncta localization during neuronal migration, the Cx43T154A–EYFP or the Cx26T135A–EYFP plasmid was co-electroporated with a plasmid expressing the red fluorescent protein tomato to visualize the cells, and followed by time-lapse microscopy. The closed pore connexin mutants were expressed in radial glia and migrating neurons in a pattern that resembled wild-type expression, but avoided the toxicity associated with wild-type connexin overexpression (Supplementary Fig. 11). Furthermore, because these mutants were sufficient to rescue migration, we can assume that they behave similarly to wild-type connexins with respect to neuronal migration.

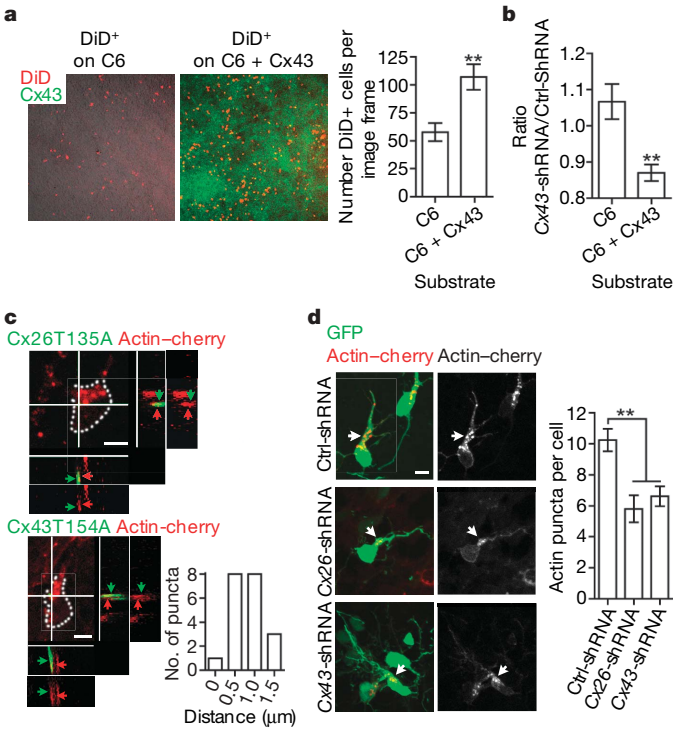

Figure 4 | Gap junctions promote cortical cell adhesion and interact with the internal actin cytoskeleton. **a**, Control DiD-labelled (red), FACS-sorted cortical cells were allowed to adhere to a glial substrate of confluent C6 or C6 + Cx43 cells. Right panel, quantification of the number of adherent DiD^+ cells per image frame (**$P \leq 0.001$, *t*-test, $n = 3$ experiments). **b**, DiD-labelled, FACS-sorted Ctrl-shRNA or *Cx43*-shRNA expressing cells were plated on a C6 or C6 + Cx43 glial substrate. The ratio of *Cx43*-shRNA to Ctrl-shRNA cells that adhered to the C6 + Cx43 substrate was about 20% less than to the C6 substrate (**$P < 0.001$, *t*-test; C6, $n = 3$ experiments; C6 + Cx43, $n = 4$ experiments). Values represent mean ± s.e.m. **c**, Cx26T135A–EYFP (top) or Cx43T154A–EYFP (bottom) puncta colocalize with actin–cherry (red) (cell bodies outlined in white), with their centre of fluorescence 0.5–1 μm apart in the *z*-plane (coloured arrows). Graph shows a frequency histogram of the distance between the centre of the puncta. **d**, Fewer actin puncta are observed in cells expressing *Cx26*-shRNA or *Cx43*-shRNA than those expressing Ctrl-shRNA (**$P < 0.001$, *t*-test; Ctrl-shRNA, $n = 37$ cells; Cx26-shRNA, $n = 21$; Cx43-shRNA, $n = 44$). Images taken at 'high resolution'. Values represent mean ± s.e.m. Scale bars, 5 μm.

The localization of Cx43T154A puncta in the branches of bifurcated leading processes was predictive of the dominant branch that would be maintained over time, and the absence of puncta was predictive of the transient branch (Fig. 5d, e, and Supplementary Movie 6). In the rare case in which a radial fibre was visible, stabilization of the branch along the fibre was observed (Fig. 5d, cell 2). When Cx26T135A was observed in the branches of bifurcated neurons, it also localized to the dominant branch (Supplementary Fig. 14a); however, Cx26T135A was not frequently present in the branches.

Cx26T135A was often localized to puncta in the cell body. Interestingly, Cx26T135A puncta in the cell body move into the dilation before the movement of the nucleus in approximately 81% of translocation events ($n = 56$) (Fig. 5f, Supplementary Movie 7 and Supplementary Fig. 14b). Cx43T154A puncta found in the cell body followed a similar pattern in approximately 57% of translocation events ($n = 24$) (Supplementary Fig. 14c). This stereotyped pattern of connexin puncta movement, which mimics the pattern of centrosome movement, indicates that gap junctions may provide the hypothesized adhesion contact associated with the centrosome in the dilation of translocating neurons[33,34]. This hypothesis is supported by the observation that Cx26T135A and Cx43T154A puncta colocalize with centrin II, where the connexin puncta are slightly offset towards the cell membrane (Fig. 5g, and Supplementary Fig. 14d). Other patterns of connexin dynamics in the trailing process and between radial fibres and neurons were also observed (Supplementary Fig. 14e, f).

Overall, the dynamics of connexin puncta localization and of shRNA electroporated cells suggest that both Cx43 and Cx26 have important roles in leading-process stabilization and somatic translocation, with Cx26 playing a more prominent part at the soma and Cx43 in the branches (Fig. 5h). Such a functional separation is consistent with the observation that Cx26 and Cx43 do not make heteromeric gap junctions, and localize to separate domains in gap junction plaques[24] (Supplementary Fig. 1).

Discussion

This study indicates that gap junctions mediate glial-guided radial migration of newborn neurons in the cortex. A recent study using conditional genetic deletion of *Cx43* indicates that gap junctions may, in addition, mediate radial migration in the hippocampus and cerebellum[35]. We find that gap junctions can promote adhesion in cortical cells, and that their adhesive but not their channel properties are necessary for migration. These dynamic gap junction adhesions between migrating neurons and radial glial fibres regulate properties of neuronal migration, including branch stabilization and nuclear translocation. The migration defect described here with acute knockdown of *Cx43* is more dramatic than the phenotype

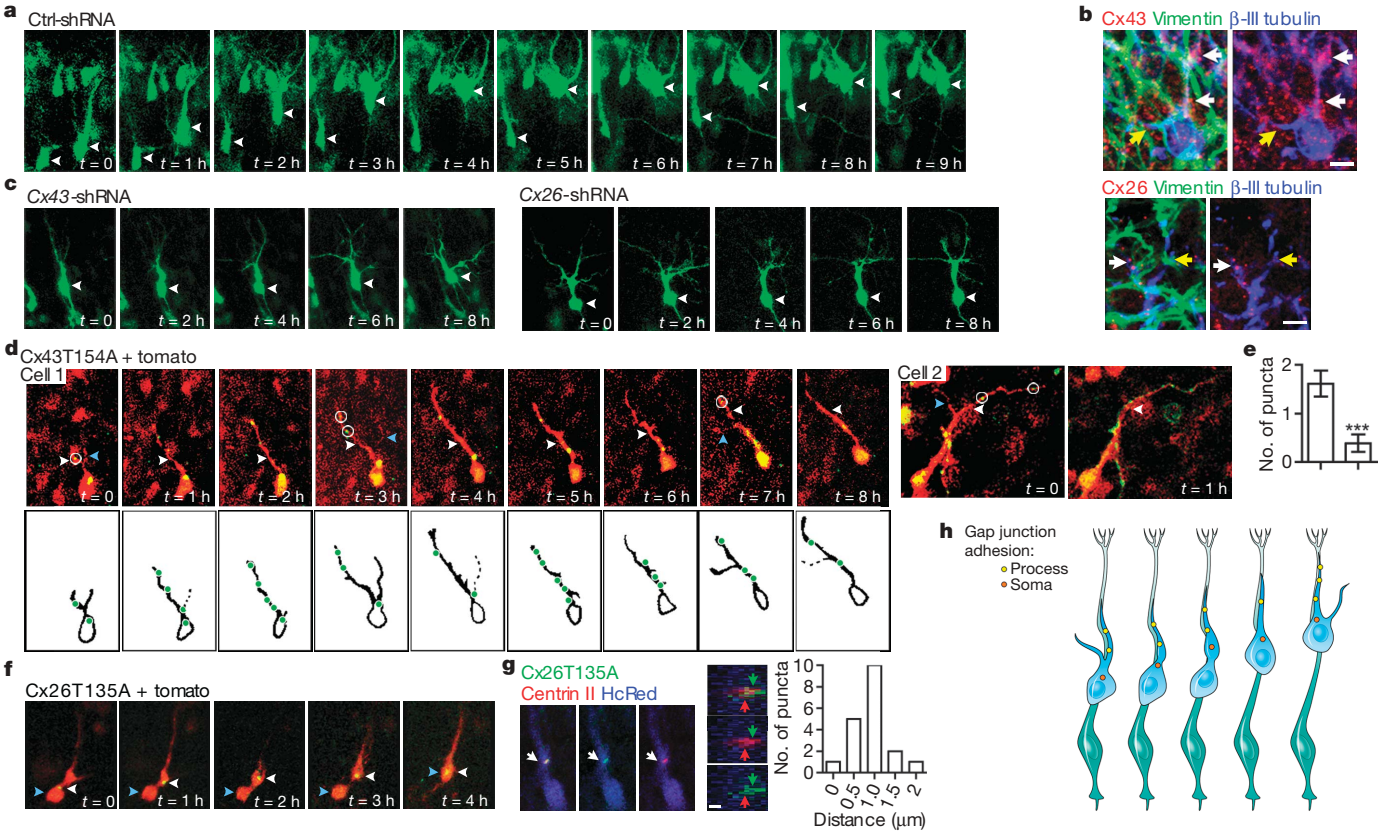

Figure 5 | Gap junction adhesions have a role in the stabilization of the migrating neuron's leading process and in the translocation of the soma. **a**, Time-lapse of two control migrating neurons (white arrowheads), demonstrating the sequence through which bifurcated neurons ($t = 0$–1 h) select a dominant leading process ($t = 1$–2 h) and translocate their soma. **b**, Immunohistochemistry for Cx43 (top) or Cx26 (bottom) in a β-III tubulin$^+$ bifurcated neuron or neuronal process (relative connexin expression, white arrows > yellow arrow). Scale bars, 5 μm. **c**, Time-lapses of neurons expressing Cx43-shRNA (left) or *Cx26*-shRNA (right) (see Supplementary Movies 4 and 5 for complete time-lapse). Neurons fail to stabilize a dominant process (note multiple transient processes), and the *Cx26*-shRNA neuron fails to translocate its soma. **d**, Time-lapses of Cx43T154A puncta in branches of bifurcated neurons. The dominant process (white arrowheads) contains numerous connexin puncta (circled in white when multiple branches), whereas transient processes (blue arrowheads) do not. **e**, The number of puncta in the dominant (Dom.) and transient (Trans.) processes (***$P \leq 0.0001$, paired *t*-test, $n = 13$). Values represent mean ± s.e.m. **f**, Time-lapse of a Cx26T135A punctum in the cell body of a migrating neuron. The punctum (white arrowhead) moves into the dilation in the leading process before the translocation of the cell body (blue arrowhead). **g**, Cx26T135A and centrin II–dsRed colocalize (white arrows) in the dilation of a migrating neuron (left panels), with their centres of fluorescence approximately 1 μm apart in the *z*-plane (middle panels, coloured arrows). Frequency histogram of the distance between the centres of the puncta (right panel). Scale bar, 1 μm. **h**, Model of gap junction adhesion dynamics in migrating neurons. Gap junction adhesive contacts stabilize the dominant leading process along radial fibres and provide an anchor in the dilation of the leading process before translocation of the soma/nucleus.

described in the *Cx43*KO mouse[14]. This may be due to developmental compensation in the genetic knockout arising from redundancy among connexins. Indeed, we show at least one other connexin, Cx26, has a very similar role in neuronal migration. Because only Cx43 has been previously implicated in cell migration, the role of Cx26 is interesting and implies that other connexins, including β1 family connexins, may be involved in migration. In addition, our work indicates that different connexins may have distinct functional roles in neural migration, with Cx26 playing a dominant role in nuclear translocation and Cx43 in branch stabilization. Furthermore, because Cx43 associates with other adhesion molecules including N-cadherin and integrin[32,36,37], it will be of interest to explore their signalling relationships. For instance, the low expression of Cx43 in the cortical plate indicates a possible interaction with integrins—which play a role in the cessation of migration[38,39]—and may aid in the detachment of neurons from radial fibres.

To our knowledge, a functional role for gap junctions based on adhesion, rather than channel activity, has not been described to date. Might gap junction adhesions have a role in other gap-junction-mediated cellular processes? It is thought that gap junction channels as well as their interactions with molecules such as p120catenin, integrin and the actin cytoskeleton are important for neural crest cell migration[32,36], and that glioblastoma invasion of the brain parenchyma requires functional gap junctions between tumour cells and astrocytes[17]. The migration of lung and skin cancer cells has also been associated with gap junction expression although no mechanism has been proposed[40,41]. In addition, the neurological disorder Charcot-Marie-Tooth syndrome, caused by mutations in Cx32, may not only result from impaired gap junction communication but also from the loss of gap junction adhesions stabilizing Schmidt–Lanterman incisures. Further studies may elucidate an important role for the adhesive properties of gap junctions in the migration of neural crest cells and cancer cells, as well as in other diseases and physiological processes associated with gap junction function.

METHODS SUMMARY

Immunohistochemistry was performed following transcardial purfusion and cryostat sectioning. Light fixing techniques and citrate antigen retrieval were used for all connexin stains. Standard confocal images were acquired on an Olympus Fluoview 300 with 1 μm steps, and 'high resolution' images were acquired on an Olympus Fluoview 1000 with 0.5 μm steps. shRNA hairpins were inserted into the pLLox3.7 construct for expression[42]. Plasmids were introduced into the *in-vivo* developing cortex by intraventricular injection of 1 μl of plasmid followed by electroporation[43]. The concentration of the shRNA plasmids was 1.7 $\mu g\,\mu l^{-1}$, and the concentration of the rescue constructs was varied according to the specified molar ratio. Intraventricular injections were carried out in E16 timed-pregnant Sprague Dawley rats. For cell transplants, electroporations were performed at E16, GFP^+ cells were dissected from electroporated corticies at E17 and dissociated, 50,000 cells per brain were intraventricularlly injected into wild-type E17 embryos, and embryos were fixed at E21. Rat Cx26 and Cx43 in the pEYFPN1 vector (Clonetech) were altered with QuickChange site-directed mutagenesis (Stratagene) to make the various connexin rescue constructs. For adhesion assays, electroporations were performed at E16 and cells were dissected at E19, FACS-sorted for GFP, labelled with Vybrant DiD (Molecular Probes), and plated on 100% confluent C6 cells (containing the TVA receptor) or C6 + Cx43 cells (containing the TVA receptor and Cx43–EYFP)[31], incubated for 30 min on a rotational shaker, and fixed. For actin or centrin co-expression experiments brains were electroporated at E16 and fixed at E19. For time-lapse imaging, electroporations were performed at E16, organotypic slice cultures were prepared[1] at E18 and allowed to equilibrate overnight before images were collected using an Olympus Fluoview 300.

Full Methods and any associated references are available in the online version of the paper at www.nature.com/nature.

Received 9 April; accepted 6 July 2007.

1. Noctor, S. C., Flint, A. C., Weissman, T. A., Dammerman, R. S. & Kriegstein, A. R. Neurons derived from radial glial cells establish radial units in neocortex. *Nature* **409,** 714–720 (2001).
2. Malatesta, P., Hartfuss, E. & Gotz, M. Isolation of radial glial cells by fluorescent-activated cell sorting reveals a neuronal lineage. *Development* **127,** 5253–5263 (2000).
3. Rakic, P. Guidance of neurons migrating to the fetal monkey neocortex. *Brain Res.* **33,** 471–476 (1971).
4. Rakic, P. Mode of cell migration to the superficial layers of fetal monkey neocortex. *J. Comp. Neurol.* **145,** 61–83 (1972).
5. Rakic, P. Specification of cerebral cortical areas. *Science* **241,** 170–176 (1988).
6. Gregory, W. A., Edmondson, J. C., Hatten, M. E. & Mason, C. A. Cytology and neuron–glial apposition of migrating cerebellar granule cells *in vitro*. *J. Neurosci.* **8,** 1728–1738 (1988).
7. Gadisseux, J. F., Kadhim, H. J., van den Bosch de Aguilar, P., Caviness, V. S. & Evrard, P. Neuron migration within the radial glial fiber system of the developing murine cerebrum: an electron microscopic autoradiographic analysis. *Brain Res. Dev. Brain Res.* **52,** 39–56 (1990).
8. Cameron, R. S. & Rakic, P. Identification of membrane proteins that comprise the plasmalemmal junction between migrating neurons and radial glial cells. *J. Neurosci.* **14,** 3139–3155 (1994).
9. Fishell, G. & Hatten, M. E. Astrotactin provides a receptor system for CNS neuronal migration. *Development* **113,** 755–765 (1991).
10. Adams, N. C., Tomoda, T., Cooper, M., Dietz, G. & Hatten, M. E. Mice that lack astrotactin have slowed neuronal migration. *Development* **129,** 965–972 (2002).
11. Anton, E. S., Marchionni, M. A., Lee, K. F. & Rakic, P. Role of GGF/neuregulin signaling in interactions between migrating neurons and radial glia in the developing cerebral cortex. *Development* **124,** 3501–3510 (1997).
12. Anton, E. S., Kreidberg, J. A. & Rakic, P. Distinct functions of α_3 and α_v integrin receptors in neuronal migration and laminar organization of the cerebral cortex. *Neuron* **22,** 277–289 (1999).
13. Nadarajah, B., Jones, A. M., Evans, W. H. & Parnavelas, J. G. Differential expression of connexins during neocortical development and neuronal circuit formation. *J. Neurosci.* **17,** 3096–3111 (1997).
14. Fushiki, S. *et al.* Changes in neuronal migration in neocortex of connexin43 null mutant mice. *J. Neuropathol. Exp. Neurol.* **62,** 304–314 (2003).
15. Huang, G. Y. *et al.* Gap junction-mediated cell–cell communication modulates mouse neural crest migration. *J. Cell Biol.* **143,** 1725–1734 (1998).
16. Lo, C. W., Waldo, K. L. & Kirby, M. L. Gap junction communication and the modulation of cardiac neural crest cells. *Trends Cardiovasc. Med.* **9,** 63–69 (1999).
17. Lin, J. H. *et al.* Connexin 43 enhances the adhesivity and mediates the invasion of malignant glioma cells. *J. Neurosci.* **22,** 4302–4311 (2002).
18. Oliveira, R. *et al.* Contribution of gap junctional communication between tumor cells and astroglia to the invasion of the brain parenchyma by human glioblastomas. *BMC Cell Biol.* **6,** 7 (2005).
19. Harris, A. L. Emerging issues of connexin channels: biophysics fills the gap. *Q. Rev. Biophys.* **34,** 325–472 (2001).
20. Dermietzel, R. *et al.* Differential expression of three gap junction proteins in developing and mature brain tissues. *Proc. Natl Acad. Sci. USA* **86,** 10148–10152 (1989).
21. Lo Turco, J. J. & Kriegstein, A. R. Clusters of coupled neuroblasts in embryonic neocortex. *Science* **252,** 563–566 (1991).
22. Bittman, K., Owens, D. F., Kriegstein, A. R. & LoTurco, J. J. Cell coupling and uncoupling in the ventricular zone of developing neocortex. *J. Neurosci.* **17,** 7037–7044 (1997).
23. Weissman, T. A., Riquelme, P. A., Ivic, L., Flint, A. C. & Kriegstein, A. R. Calcium waves propagate through radial glial cells and modulate proliferation in the developing neocortex. *Neuron* **43,** 647–661 (2004).
24. Falk, M. M. Connexin-specific distribution within gap junctions revealed in living cells. *J. Cell Sci.* **113,** 4109–4120 (2000).
25. Beahm, D. L. *et al.* Mutation of a conserved threonine in the third transmembrane helix of α- and β-connexins creates a dominant-negative closed gap junction channel. *J. Biol. Chem.* **281,** 7994–8009 (2006).
26. Komuro, H. & Rakic, P. Intracellular Ca^{2+} fluctuations modulate the rate of neuronal migration. *Neuron* **17,** 275–285 (1996).
27. Giepmans, B. N. & Moolenaar, W. H. The gap junction protein connexin43 interacts with the second PDZ domain of the zona occludens-1 protein. *Curr. Biol.* **8,** 931–934 (1998).
28. Lin, R., Warn-Cramer, B. J., Kurata, W. E. & Lau, A. F. v-Src phosphorylation of connexin 43 on Tyr247 and Tyr265 disrupts gap junctional communication. *J. Cell Biol.* **154,** 815–827 (2001).
29. Giepmans, B. N. *et al.* Gap junction protein connexin-43 interacts directly with microtubules. *Curr. Biol.* **11,** 1364–1368 (2001).
30. Naus, C. C., Bechberger, J. F., Caveney, S. & Wilson, J. X. Expression of gap junction genes in astrocytes and C6 glioma cells. *Neurosci. Lett.* **126,** 33–36 (1991).
31. Lai, A. *et al.* Oculodentodigital dysplasia connexin43 mutations result in non-functional connexin hemichannels and gap junctions in C6 glioma cells. *J. Cell Sci.* **119,** 532–541 (2006).
32. Xu, X., Francis, R., Wei, C. J., Linask, K. L. & Lo, C. W. Connexin 43-mediated modulation of polarized cell movement and the directional migration of cardiac neural crest cells. *Development* **133,** 3629–3639 (2006).
33. Schaar, B. T. & McConnell, S. K. Cytoskeletal coordination during neuronal migration. *Proc. Natl Acad. Sci. USA* **102,** 13652–13657 (2005).

34. Tsai, J. W., Bremner, K. H. & Vallee, R. B. Dual subcellular roles for LIS1 and dynein in radial neuronal migration in live brain tissue. *Nature Neurosci.* **10**, 970–979; advance online publication, doi:10.1038/nn1934 (8 July 2007).
35. Wiencken-Barger, A. E., Djukic, B., Casper, K. B. & McCarthy, K. D. A role for Connexin43 during neurodevelopment. *Glia* **55,** 675–686 (2007).
36. Xu, X. *et al.* Modulation of mouse neural crest cell motility by N-cadherin and connexin 43 gap junctions. *J. Cell Biol.* **154,** 217–230 (2001).
37. Meyer, R. A., Laird, D. W., Revel, J. P. & Johnson, R. G. Inhibition of gap junction and adherens junction assembly by connexin and A-CAM antibodies. *J. Cell Biol.* **119,** 179–189 (1992).
38. Dulabon, L. *et al.* Reelin binds α3β1 integrin and inhibits neuronal migration. *Neuron* **27,** 33–44 (2000).
39. Schmid, R. S., Jo, R., Shelton, S., Kreidberg, J. A. & Anton, E. S. Reelin, integrin and DAB1 interactions during embryonic cerebral cortical development. *Cereb. Cortex* **15,** 1632–1636 (2005).
40. el-Sabban, M. E. & Pauli, B. U. Adhesion-mediated gap junctional communication between lung-metastatatic cancer cells and endothelium. *Invasion Metastasis* **14,** 164–176 (1994).
41. Ito, A. *et al.* A role for heterologous gap junctions between melanoma and endothelial cells in metastasis. *J. Clin. Invest.* **105,** 1189–1197 (2000).
42. Lois, C., Hong, E. J., Pease, S., Brown, E. J. & Baltimore, D. Germline transmission and tissue-specific expression of transgenes delivered by lentiviral vectors. *Science* **295,** 868–872 (2002).
43. Saito, T. & Nakatsuji, N. Efficient gene transfer into the embryonic mouse brain using *in vivo* electroporation. *Dev. Biol.* **240,** 237–246 (2001).

Supplementary Information is linked to the online version of the paper at www.nature.com/nature.

Acknowledgements We are grateful for ideas arising from discussions with G.M. Elias, members of the Kriegstein Laboratory, A. Alvarez-Buylla, J. L. Rubensetin and S. J. Pleasure, as well as manuscript and figure editing by G.M. Elias. We thank D. Laird for connexin plasmids, A. Lai for C6 cell lines, K. Hu for the actin–cherry plasmid, R. Vallee for the centrin II–dsRed plasmid, and W. Walantus, J. Agudelo and T. Calcagni for technical support. Artwork in Fig. 5h is by K. X. Probst. This work was supported by grants from the National Institutes of Health (to A.R.K.), the Sandler Family and Genentech Graduate Fellowship (to L.A.B.E.), the California Institute for Regenerative Medicine Graduate Fellowship (to L.A.B.E.), and the J.G. Bowes Research Fund.

Author Contributions L.A.B.E. conceived of and carried out all experiments except as noted below. D.D.W. developed methods for and carried out the cell transplant/cell autonomy experiments and the whole-cell patch clamp recordings in C6 cells. A.R.K., as the principle investigator, provided conceptual and technical guidance for all aspects of the project. L.A.B.E. wrote the manuscript. All authors discussed the results/experiments and revised/edited the manuscript.

Author Information Reprints and permissions information is available at www.nature.com/reprints. The authors declare no competing financial interests. Correspondence and requests for materials should be addressed to L.A.B.E. (EliasL@stemcell.ucsf.edu) or A.R.K. (KriegsteinA@stemcell.ucsf.edu).

METHODS

Immunohistochemistry and imaging. Embryos were fixed by transcardial purfusion with PBS followed by 4% paraformaldehyde in PBS (PFA). A subsequent perfusion of PBS was performed in embryos used for Cx26/43 staining. Brains were post-fixed over night (except for Cx26/43 staining), dehydrated in 20% and 30% sucrose, frozen, and cryostat sectioned at 14 μm (except for Cx26/43 staining, which used 10 μm). For endogenous knockdown assays, dissociated cortical cells were plated on Poly-L-Lysine coated coverslips, allowed to adhere for 2 h, and fixed in PFA (10 min). Citrate antigen retrieval was preformed for Cx26/43 and Ki67 staining. Blocking solution contained 2% gelatin, 10% serum and 1% Triton-X-100 in PBS. Sections/cells were incubated overnight in primary antibodies: rabbit anti-Cx43 (1:50, Zymed), mouse anti-Cx43 (1:50, Zymed), rabbit anti-Cx26 (1:25, Zymed SI-2800), chicken anti-vimentin (1:1,000, Chemicon), mouse anti-β-III tubulin (TUJ1) (1:200, Covance), chicken anti-GFP (1:500, Aves Labs), rabbit anti-Ki67 (1:1,000, Novocastra), mouse anti-bromodeoxyuridine Alexa Flour 647 (1:50, Molecular Probes), mouse anti-nestin (1:100, Chemicon), rabbit anti ZO-1 (1:100, Zymed), mouse anti N-cadherin (1:100, Zymed), and mouse anti β1-integrin (1:100, BD Transduction Laboratories). TUNEL staining was performed using TMR red Cell Death Detection Kit (Roche). Secondary antibodies included Alexa 488/568 conjugates (Molecular Probes) or Cy3/Cy5 conjugates (Jackson). Standard images were acquired on an Olympus Fluoview 300 laser-scanning confocal microscope. 'Standard' images of connexin staining represent collapsed ≤ 3 μm stacks collected at 1-μm steps, and other standard images represent single optical sections. 'High resolution' images were collected on an Olympus Fluoview 1000 at 0.5-μm steps. Images were analysed using Photoshop 7.0.

Plasmid constructs. ShRNA oligonucleotides were inserted into the dual promoter construct pLLox3.7 for expression under the U6 promoter (EGFP was expressed under the CMV promoter)[42]. The following target sequences were used for *Cx26*, TCTGGAATTTGCATCCTGCTA (alternative target: GCAGCGTCTGGTGAAGTGTAA); and *Cx43*, GCAATTACAACAAGCAAGCTA (alternative target: GGCTTGCTGAGAACCTACATCATCA). The control shRNA oliognucleotiedes with three point mutations (underlined) were as follows for Cx26, TCTTGAATATGCATCGTGCTA; and Cx43, GTAATTGCAACAAGAAAGCTA. The following target sequences were used for the P2Y1 receptor: *P2Y1*-shRNA(2) GGAGTGAGGCCAATTTACA, *P2Y1*-shRNA(3) GAGTACCTGCGAAGTTATT.

Rat Cx26 and Cx43 clones in the pEYFP-N1 vector (Clonetech) were a gift of D. Laird. QuickChange site-directed mutagenesis (Stratagene) was used to introduce the following point mutations as underlined: Cx26CM, CTCTGTGTCCGGAATCTGCATACTGCTCAACATCACAGAGCTGTG; Cx43CM, CCTCGTGCCGGAATTATAACAAACAAGCCAGCGAGCAAAACTGGG; Cx43C61S, CTCAACAACCTGGCTCCGAAAACGTCTGCTATGAC; Cx26T135A, TCCCTGTGGTGGGCCTACACCACCAGC; Cx43T54A, GGCTTGCTGAGAGCCTACATCATCAGCATCC; Cx26 1-216, ATCACAGAGCTGTGCTATCTGTTCATTA**GAATTC**GCTCAGGGAAGTCC; Cx43 1–238, TTCAAAGGCGTTAA**GGATCC**CGTGAAGGGAAG (introduced restriction site in bold). The P2Y1 receptor was cloned with the following primers: AGCTCGAGTGCCTGAGTTGGAAAGAAG (sense), TCGAATTCGGGCGTAGTCGGGCACGTCGTAGGGGTACAAACTTGTGTCTCCGTT (antisense), and inserted into the pEYFPN1 vector (Clonetech) using the *Xho*1 and *Eco*R1 restritction sites. The antisense primer introduced a haemagglutinin (HA) tag and removed the stop codon.

Cell transfections and western blots. Western blots were performed on Cos-7 cells transfected with FuGENE6 transfection reagent (Roche) with 1 μg of DNA, 200 μl Opti MEM and 5 μl FuGENE6 per 35 mm dish. Samples were collected 3 days post transfection in RIPA buffer (150 mM NaCl, 0.1%SDS, 1% triton X100, 50 mM TrisHCl pH 6.8, 1 mM EDTA, 0.5% deoxycholate, 10% glycerol) plus protease inhibitors, normalized for protein concentration, denatured at 37 °C for 30 min in 4× loading buffer (6 mM Tris pH 6.8, 5% β-Mercaptoethanol, 2% SDS, .05% bromophenol blue), and run on Criterion Precast 12.5% Tris-HCl gels (Bio-Rad). Membranes were probed with rabbit anti-Cx43 (1:1,000, Zymed) or rabbit anti-Cx26 (1:2,000, Zymed 71-0500) followed by anti-rabbit peroxidase conjugate (1:2,000, Sigma) or with mouse anti-HA peroxidase for P2Y1–HA detection (1:2,000, Sigma H 6533). All blots were stripped and re-probed with mouse anti-γ-tubulin (1:500, Sigma) and anti-mouse peroxidase conjugate (1:400, Sigma). For quantification, all western blots were normalized to the levels of the loading control γ-tubulin and band intensity was measured in Photoshop. C6 cells were transfected with FuGENE6 transfection reagent (Roche) with 0.3 μg of DNA, 20 μl Opti MEM and 2 μl FuGENE6 per 16 mm dish.

***In-utero* injection and electroporation/cell transplants.** Animals were maintained according to protocols approved by the Institutional Animal Care and Use Committee at UCSF. Plasmids were introduced into the developing cortex *in vivo* by intraventricular injection and electroporation[43]. Intraventricular injections were carried out in E16 timed-pregnant Sprague Dawley rats as previously described[1]. Electroporations were performed using an Electro Square Porator ECM830 (Genetronics) (5 pulses, 50 V, 100 ms, 1-s interval). DNA was prepared in endotoxin-free conditions and 1 μl was injected per brain at the following concentrations: shRNA constructs, 1.7 μg μl^{-1}; rescue constructs, at a molar ratio of 0.67:1 (Cx26 rescue construct: *Cx26*-shRNA) or 0.45:1 (Cx43 rescue construct: *Cx43*-shRNA); Cx26T135A and Cx43T154A 1.7 μg μl^{-1}; Tomato 1 μg μl^{-1}; actin–cherry 1.7 μg μl^{-1}; centrin II–dsRed 2.0 μg μl^{-1}; HcRed 2.5 μg μl^{-1}. For analysis of endogenous knockdown, electroporations were performed at E16 and cortices were dissociated at E18, allowed to adhere in culture for 2 h, fixed and stained. For cell transplants, electroporations were performed at E16, GFP^{+} cells were dissected from electroporated corticies at E17 in ACSF(125 mM NaCl, 2.5 mM KCl, 1 mM $MgCl_2$, 2 mM $CaCl_2$, 1.25 mM NaH_2PO_4, 25 mM $NaHCO_3$ and 20 mM glucose), the cells were dissociated and resuspended in culture media containing 25% Hanks BBS, 47% Basal Medium Eagle (Gibco), 5% Fetal bovine serum, 1X Pen/Strep, 0.66% glucose, 1% N2-supplement (Invitrogen). Fifty-thousand cells per brain were intraventricularly injected into wild-type E17 embryos, and embryos were fixed at E21. The video protocol in ref. 44 fully explains the *in utero* intraventricular injections and electroporations.

Quantification of cell distribution. The shRNA cell distribution phenotype was quantified by taking a total of 20 evenly spaced rostral to caudal sections per brain from 3 brains per condition. A threshold was applied in Photoshop and the fraction of cells in each of 5 rows of equal area (A–E) stacked parallel to the ventricular zone surface was quantified in each slice and then averaged across slices. The *Cx43*-shRNA rescue experiments were quantified in a similar manner by counting the fraction of cells in the cortical plate (layers C, D and E) in 10 rostral to caudal sections per brain for 4–6 brains per condition. For the *Cx26*-shRNA rescue experiments, 5 medial to caudal sections per brain for 4–6 brains per condition were quantified. For transplant experiments, confocal stacks of all sections with cells that integrated into the cortex were collected and the number of cells in each area (A–E) was counted. All quantifications were performed in a blind manner.

Cell sorting. Electroporations were performed at E16 and cells were dissected at E19 in ACSF. Cells were transferred to PBS 2%FBS immediately before sorting and kept on ice. Cells were sorted for GFP on a FACSAria (Becton Dickinson) using a 100 μm nosel, 488 laser with the 530/30 filter, and were collected in culture media. Collected cells were labelled with Vybrant DiD cell labelling solution (Molecular Probes) in serum-free culture media for 20 min and washed according to the instructed protocol. Ten-thousand cells were plated per well of 100% confluent C6 cells grown on 24-well collagen biocoat plates (Becton Dickinson). C6 (containing the TVA receptor) and C6 + Cx43 (containing the TVA receptor and Cx43–EYFP) cells were a gift of A. Lai[31]. Cells were incubated for 30 min, with shaking at 250 rpm, and then washed 4 times with PBS, and fixed. Each experiment included three or more wells of each condition. Five pictures of each well were taken (middle, right, left, top, bottom), and quantifications were carried out in a blind manner.

Time-lapse imaging. Electroporations were performed at E16 and 300-μm thick vibratome sections were prepared at E18 in ACSF. Slices were plated on Millicell-CM inserts (Millipore) in culture medium and allowed to equilibrate overnight before imaging. Confocal images, were collected on the Olympus Fluoview 300 at 2–5-μm steps (to minimize bleaching) every hour for 8–10 h. Stacks containing the cell of interest were collapsed and analysed in Photoshop. The video protocol in ref. 45 fully explains the slice culture system used for time-lapse experiments.

44. Walantus, W., Elias, L. & Kriegstein, A. R. *In utero* intraventricular injection and electroporation of E16 rat embryos. *J. Visualized Exp.* **6** ⟨http://www.jove.com/index/Details.stp?ID=236&VID=222⟩ (2007).
45. Elias, L. & Kriegstein, A. R. Organotypic slice culture of E18 rat brains. *J. Visualized Exp.* **6** ⟨http://www.jove.com/index/Details.stp?ID=235&VID=221⟩ (2007).